# ENABLING ADAPTIVE DETACHMENT CONTROL: NOVEL INSIGHTS FROM CALIBRATION-FREE X-POINT PHASE DIFFERENCE

Yue Yu Institute of Plasma Physics, Chinese Academy of Sciences Hefei, China Email: yue.yul@ipp.ac.cn

Liang Wang, Yan-Min Duan, Wei Gao, Guo-Sheng Xu Institute of Plasma Physics, Chinese Academy of Sciences Hefei, China

#### **Abstract**

Divertor detachment monitoring is essential for sustained tokamak operation under reactor-relevant conditions, yet remains challenging with conventional diagnostics. The paper proposes a physics-informed framework, termed X-Point Ionization and Radiation Interface Structure (X-IRIS), for robust detachment assessment. By leveraging the relative phase shift between two sightlines adjacent to the X-point, X-IRIS provides a calibration-free metric of detachment states, independent of direct electron-temperature measurements near the divertor targets. The approach quantifies both the direction and magnitude of turbulent filament transport between the X-point and divertor, revealing the link between cross-separatrix flow asymmetry and detachment states. X-IRIS thus presents a promising solution for non-invasive detachment monitoring in next-generation tokamak reactors.

### 1. INTRODUCTION

Fusion reactors hold great promise for clean energy, but their safe and stable operation hinges on effective power exhaust, particularly through the divertor, which must operate under strict heat load limits (<10 MWm<sup>-2</sup>) and thus requires partial detachment to reduce power deposition near the separatrix [1,2]. This detachment process is closely linked to X-point physics, where plasma cooling via radiation and ionization occurs, influenced by mesoscale turbulent filaments that transport energy across the separatrix and regulate detachment onset and sustainment [3–7]. However, monitoring and controlling this process remains challenging due to limitations in conventional diagnostics: Langmuir probes are prone to damage under high heat flux [8,9], while optical diagnostics suffer from overexposure and complex data inversion [10,11]. To overcome these issues, a novel physics-informed framework, the X-point Ionization-Radiation Interface Structure (X-IRIS), is introduced. X-IRIS utilizes widely available diagnostics and statistical signal analysis to establish a calibration-free metric for detachment, enabling non-invasive assessment of cross-separatrix turbulence and its impact on divertor conditions, with potential for improving resilience against large edge-localized modes and enhancing detachment control in future burning plasmas.

# 2. EXPERIMENTAL CONDITIONS

This study employs data from the Experimental Advanced Superconducting Tokamak (EAST), a device dedicated to steady-state operation and equipped with prototype systems relevant to next-generation reactors, thereby enhancing the validity and generalizability of the findings [12]. While prior EAST experiments often focused on high- $\beta$  scenarios ( $q_{95} = 6-8$ ), this work shifts emphasis to discharges with  $q_{95}$  between 2 and 5, representative of hybrid and advanced operational regimes. Both neutral beam injection (NBI) and radio-frequency (RF) heating—alone and in combination—are included to account for differing heating physics. The analysis is restricted to the lower single-null (LSN) magnetic configuration, which is widely adopted in tokamaks. Diagnostics include the absolute extreme ultraviolet (AXUV) and filterscope systems, mounted in nearly toroidally opposite ports (Figure 1), providing measurements of total radiated power and deuterium-alpha emission for neutral recycling monitoring, respectively [13,14]. Three sightlines from each system, including one intersecting the X-point (highlighted in Figure 2), are used to probe X-point turbulence. Complementary Langmuir probes on the lower divertor targets serve as conventional detachment indicators [15], positioned between the spectral diagnostic ports to minimize toroidal asymmetry effects.

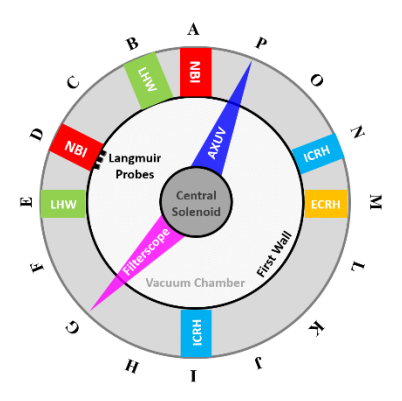


FIG. 1. Toroidal layouts of the utilized heating systems and diagnostics.

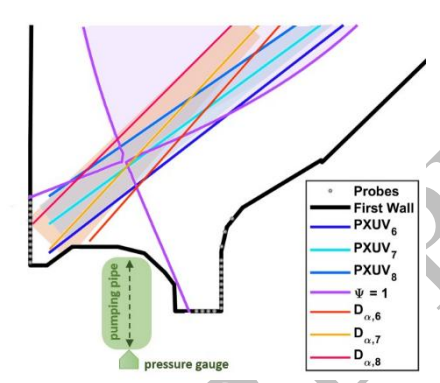


FIG. 2. Poloidal diagram of the detected areas of interest.

### 3. DETAILS OF X-IRIS

### 3.1. Framework rationale

The conceptual foundation of X-IRIS draws an analogy to cooling boiling water by blowing or stirring, which enhances heat transfer and drives the system toward a more uniform, higher-entropy state. Similarly, X-point turbulence facilitates cross-separatrix transport of particles and heat, promoting energy dissipation before power reaches the divertor target. The closed-flux region and scrape-off layer (SOL) act as interconnected systems with distinct profiles, separated by the separatrix. Turbulent fluctuations driven by entropy increase propagate across this boundary, and the resulting phase difference between adjacent diagnostic sightlines reflects the intensity of turbulent energy exchange. A larger phase difference indicates strong upstream dissipation and a more uniform, high-entropy divertor state—consistent with detachment—while a small phase difference signifies inefficient dissipation and a localized, low-entropy heat flux, characteristic of attached conditions. Thus, the phase difference serves as a dynamic indicator of detachment progression.

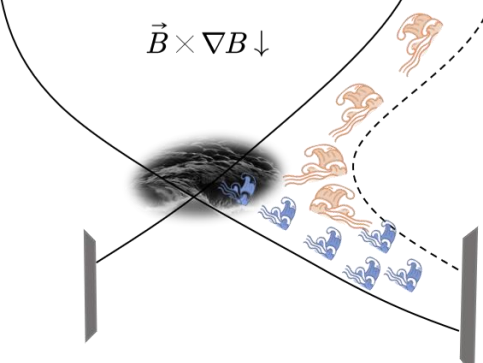


FIG. 3. Schematic of X-IRIS.

In discharges with  $q_{95} = 2-5$ , large edge-localized modes (ELMs) are prevalent [16], manifesting as filamentary bursts propagating along field lines. Within a filament-based framework [17], the divertor leg supports

two counter-flowing components: upstream-connected filaments (UCFs) moving toward the target and divertor-local filaments (DLFs) propagating toward the X-point, as shown in Figure 3. At lower temperatures, reduced ion gyroradius ( $\rho_i$ ) allows UCFs to pass through the X-point, while lower sound speed ( $c_s$ ) and weaker radial electric fields ( $E_r$ ) prolong their residence time. This leads to UCF accumulation, suppression of DLF regeneration, enhanced cross-field diffusion, and broadening of the heat flux footprint ( $\lambda_q$ ). In contrast, at higher temperatures, increased  $\rho_i$  causes UCFs to be intercepted at the X-point, while higher  $c_s$  and stronger  $E_r$  reduce residence time, fragmenting UCFs and advecting them rapidly toward the target, thereby inhibiting DLF formation. This results in a narrower  $\lambda_q$ . Consequently, DLF-dominated SOL dynamics correlate with hotter, attached divertor conditions and reduced core-SOL coupling, leading to smaller phase differences near the X-point.

While ELM-induced filaments are the primary source of turbulence in the divertor leg, impurity transport significantly influences overall behavior. The filterscope system monitors  $D\alpha$  emission, which reflects filament strength and incorporates ionization-recombination dynamics, while AXUV diodes measure impurity radiation, providing complementary information on radiative dissipation. A consistent phase asymmetry is observed: the AXUV (radiation) signal typically leads on the divertor side but lags on the core side, whereas the  $D\alpha$  signal exhibits the opposite trend. This discrepancy arises from local plasma conditions—on the divertor side, lower temperatures, shorter connection lengths, and enhanced impurity deposition yield a faster radiative response, while near the X-point on the core side, higher temperatures promote rapid ionization and neutral consumption, causing the  $D\alpha$  signal to lead in phase due to its sensitivity to filament sources.

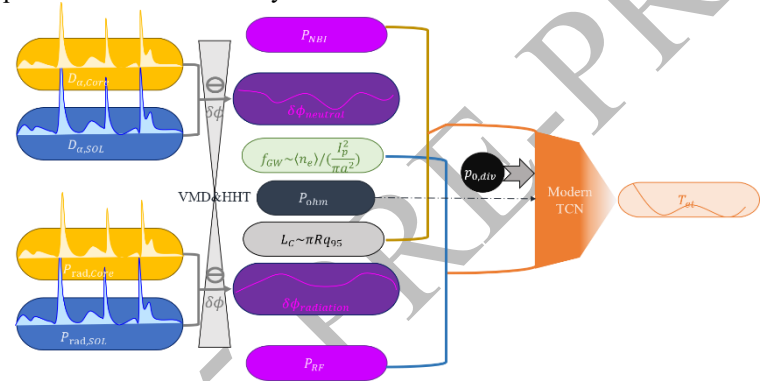


FIG. 4. Framework of X-IRIS.

However, the phase difference between Da and AXUV signals alone is insufficient for robust detachment assessment; the connection length between upstream and divertor regions must also be accounted for, as it affects the evolution of both divertor-local (DLFs) and upstream-connected filaments (UCFs). The stability of radiative structures—such as X-point radiators (XPR) or MARFEs—is critical in shaping X-point turbulence. As noted by Stroth, the XPR-MARFE transition is strongly influenced by neutral particles [3], a result supported by simulations [18]. Therefore, the analysis incorporates the normalized Greenwald density fraction and neutral pressure below the divertor baffle. Additionally, RF and neutral beam injection (NBI) heating powers are treated separately, following Yu's findings [19], and ohmic power is included to improve long-pulse operational forecasting. Together, these components constitute the complete X-IRIS framework, as summarized in Figure 4.

To strengthen the rationale for feature selection, the maximum information coefficient (MIC) [20] was computed between each input feature and the output variable. The results validate the relevance of the selected features, confirming that the chosen variables are well justified.

## 3.2. Dataset

To ensure model generalizability across diverse operational scenarios, the dataset includes a broad range of auxiliary heating combinations used in EAST, encompassing various configurations of electron cyclotron resonance heating (ECRH), lower hybrid wave (LHW), ion cyclotron resonance heating (ICRH), and neutral beam injection (NBI). Only discharges with ICRH-only, ICRH combined with a single additional heating method (ECRH, LHW, or NBI), or ICRH with both ECRH and LHW were excluded. The dataset was stratified to maintain consistent distributions of all input variables—including heating powers, density, and connection length—across training, validation, and test sets. The target variable, derived from Langmuir probe measurements, is restricted to the 3–110 eV range where probe data are reliable, with its distribution balanced across subsets. The final dataset

comprises 189 discharges: 134 for training, 41 for validation, and 14 for testing, corresponding to approximately 304 s, 85 s, and 35 s of cleaned temporal data, respectively.

## 3.3. Model Topology

While qualitative physical insights are valuable, they offer limited utility for reactor operation without quantitative formulation. Deriving a first-principles analytical model encompassing the full complexity of X-point turbulence and detachment dynamics is infeasible. In this context, artificial intelligence provides a powerful means to extract underlying patterns from experimental data. After evaluating several architectures, a convolutional timeseries model, ModernTCN, was selected for its efficiency and effectiveness [21]. As illustrated in Figure 5, ModernTCN emphasizes conceptual and structural simplicity, achieving a favorable balance between performance and computational cost. Its large receptive field enables the capture of long-range temporal dependencies with relatively few convolutional layers, yielding accuracy comparable to attention-based models like Transformers, but with fewer parameters and faster inference. Importantly, the architecture decouples the modeling of temporal dynamics within individual variables from the learning of inter-variable relationships, enhancing both representational power and model interpretability. For full technical details, the reader is referred to the original work [21].

FIG. 5. Workflow of ModernTCN.

## 4. APPLICATIONS OF X-IRIS

To evaluate the performance of the proposed framework, this section analyzes representative discharges under various commonly employed heating schemes and their associated divertor conditions. The electron temperature referenced is the peak value measured at the lower outer divertor targets. The model utilizes and presents the estimated absorbed heating power as input for prediction.

Neutral beam injection (NBI) simultaneously fuels and heats the plasma through high-energy neutral particles, but its impact can be either beneficial or detrimental depending on injection timing and intensity; uncontrolled NBI may trigger instabilities leading to disruptions, underscoring the critical need for real-time monitoring of divertor heat loads. As shown in Figure 6, when RF heating initiates diverted plasma and NBI power is gradually increased, rising neutral pressure and decreasing electron temperature at the lower outer divertor target indicate a transition toward a cooled, partially detached state, accompanied by fluctuating phase differences signaling active X-point energy dissipation. When NBI power is held constant, neutral pressure drops due to pumping, and the divertor temperature gradually recovers, demonstrating the physical consistency and monitoring capability of the X-IRIS framework.

In contrast, RF heating—driven by wave-particle interactions—naturally induces plasma fluctuations. Figure 7 shows that even at nearly constant RF power, variable absorption efficiency leads to transient, irregular dynamics in the X-point region, reflected in phase differences and correlated with divertor electron temperature variations. This supports the conclusion that phase difference is a dominant factor in determining divertor heat load, with RF-induced uncertainty posing control challenges.

Given the dual nature of NBI and the destabilizing potential of RF heating, their combined application is of particular interest. Previous studies report synergistic effects broadening the scrape-off layer [19]. Figure 8 reveals that under constant NBI and RF power, despite noisy phase signals, the divertor remains stably detached, and changes in RF power have little effect on neutral pressure or temperature—indicating that NBI drives cooling

while RF-induced turbulence persists. However, when RF power is modulated at constant NBI (Figure 9), self-sustained divertor oscillations emerge [22], likely due to an unfavorable NBI-to-RF power ratio. When RF dominates, NBI's stabilizing effect weakens, and RF-induced electric fields may disrupt drift-mediated particle exchange between inner and outer divertors, degrading the high-recycling regime. These results highlight the necessity of actively regulating the NBI-to-RF power ratio to maintain stable, safe divertor operation in future reactors.

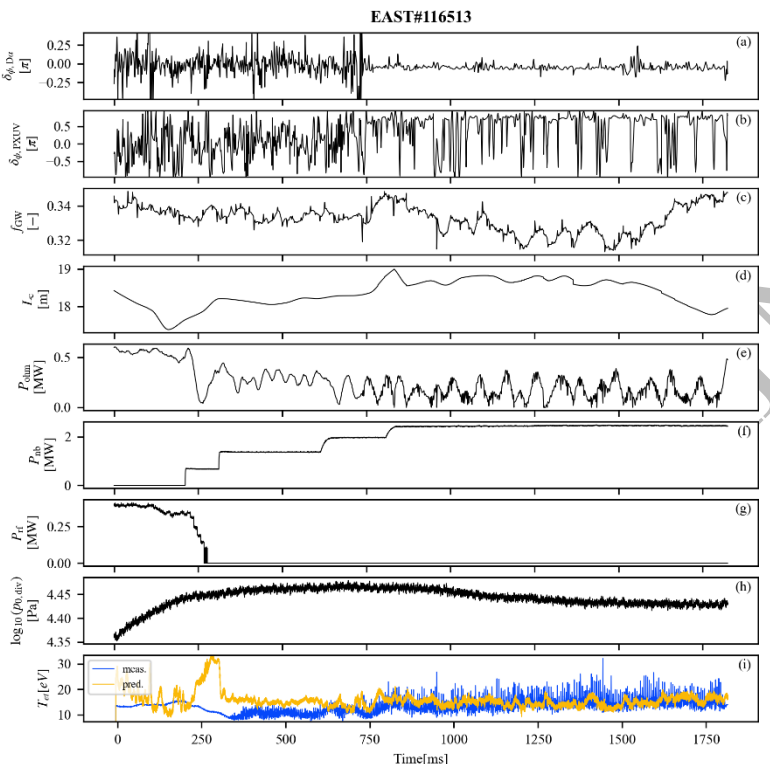


FIG. 6. Segments of an NBI dominant discharge applied with X-IRIS. EAST#115932

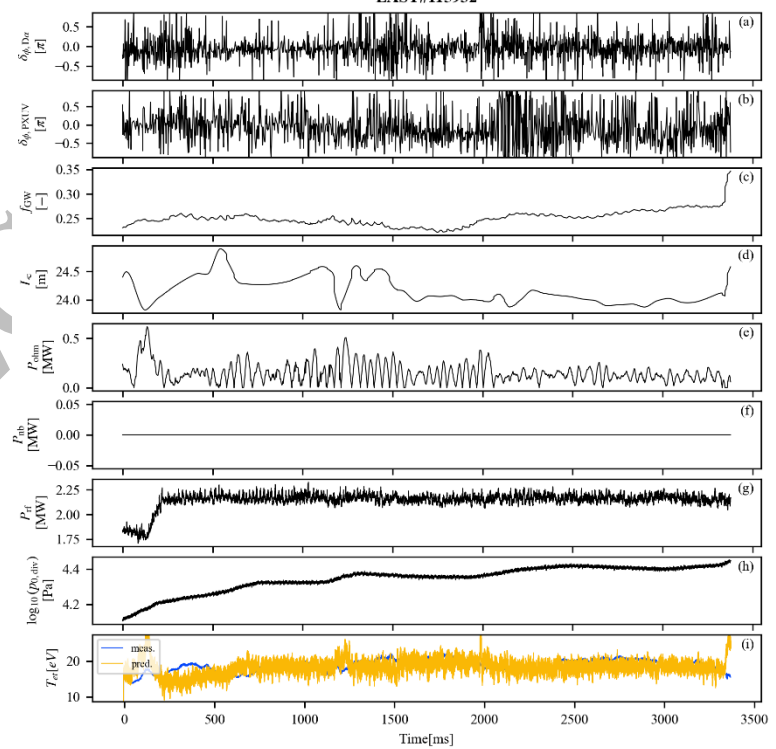


FIG. 7. Segments of a pure RF-heating discharge applied with X-IRIS.

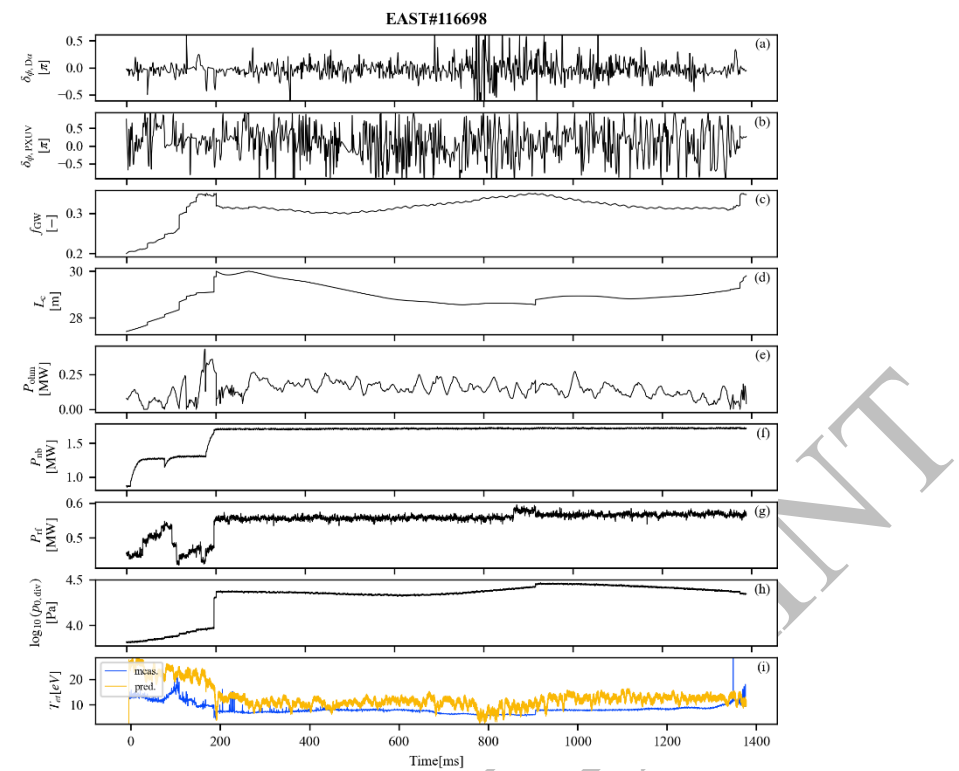


FIG. 8. Segments of a stable NBI and RF synergetic heating discharge applied with X-IRIS.

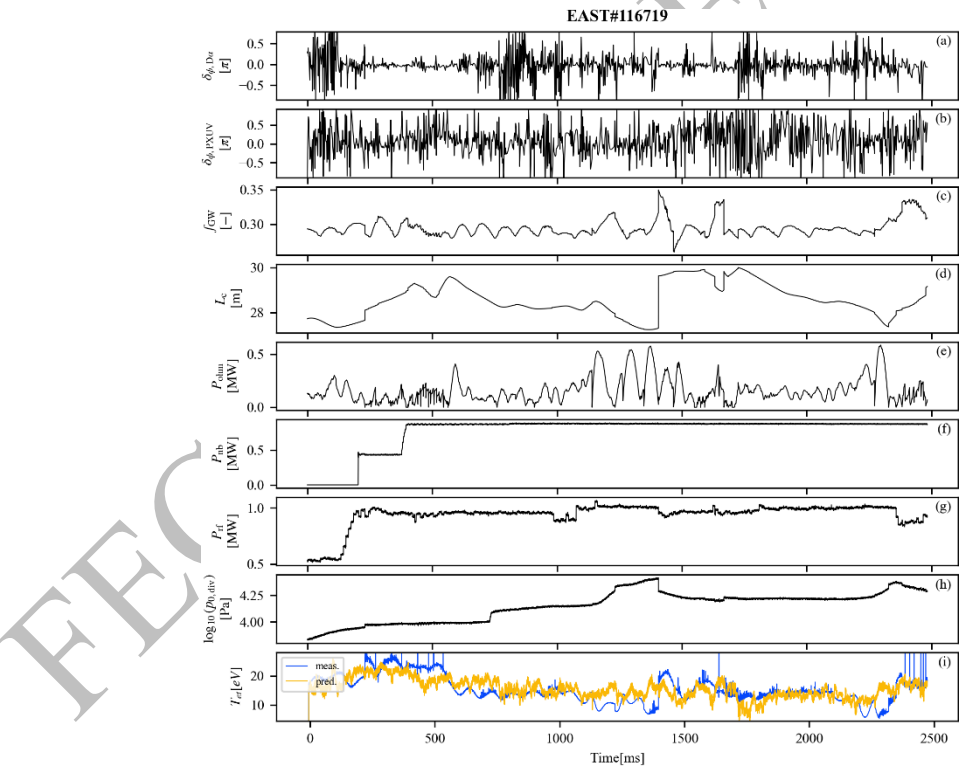


FIG. 9. Segments of an unsteady NBI and RF synergetic heating discharge applied with X-IRIS.

# 5. CONCLUSIONS AND OUTLOOK

This study addresses the challenge of monitoring divertor heat load under extreme fusion reactor conditions, particularly during large ELMy H-mode operation. A physics-informed deep learning framework, X-IRIS, is developed for broad applicability and practical deployment. By analyzing phase shifts in non-invasive diagnostic signals—specifically from AXUV and filterscope systems—X-IRIS captures X-point turbulence to track local entropy evolution and infer energy dissipation in the divertor region, enabling real-time assessment of divertor

conditions. The model was rigorously trained and validated across diverse heating schemes on EAST, demonstrating robust performance. It further elucidates the distinct roles of NBI and RF heating: while NBI promotes divertor cooling, RF heating introduces fluctuations that affect stability, highlighting the critical need to optimize the NBI-to-RF power ratio for synergistic heat load reduction.

Conventional methods for X-point turbulence monitoring, such as bolometric inversion for detachment control, are often computationally demanding and sensitive to calibration errors. In contrast, X-IRIS introduces a novel approach based on phase differences between poloidally arranged spectroscopic sightlines, offering a quantitative, calibration-free assessment of energy dissipation dynamics near the X-point. By avoiding reliance on absolute radiometric calibration, X-IRIS represents a pioneering step toward calibration-independent monitoring in fusion science. To enhance generalizability for future reactors, integration of data from additional devices is planned. Future work will focus on developing a more compact, efficient, and powerful version of the framework for real-time control applications.

#### **ACKNOWLEDGEMENTS**

This work was supported by the National Natural Science Foundation of China No.12275312 and the HFIPS Director's Fund No. BJPY2023A05. Furthermore, the authors would like to appreciate the staff at EAST (https://cstr.cn/31130.02.EAST) for technical support and data assistance.

#### REFERENCES

- [1] Pitts R A et al., 2019 Physics basis for the first ITER tungsten divertor Nucl. Mater. Energy 20 100696
- [2] Kallenbach A et al., 2015 Partial detachment of high-power discharges in ASDEX Upgrade Nucl. Fusion 55 053026
- [3] Stroth U et al., 2022 Model for access and stability of the X-point radiator and the threshold for marfes in tokamak plasmas Nucl. Fusion 62 076008
- [4] KRASHENINNIKOV S I et al., 2008 Recent theoretical progress in understanding coherent structures in edge and SOL turbulence J. Plasma Phys. 74 679–717
- [5] Rudakov D L et al., 2005 Far SOL transport and main wall plasma interaction in DIII-D Nucl. Fusion 45 1589–99
- [6] Carralero D et al., 2018 On the role of filaments in perpendicular heat transport at the scrape-off layer Nucl. Fusion 58 096015
- [7] Eich T et al., 2020 Turbulence driven widening of the near-SOL power width in ASDEX Upgrade H-Mode discharges Nucl. Fusion 60 056016
- [8] Wang L et al., 2021 Progress of Divertor Heat and Particle Flux Control in EAST for Advanced Steady-State Operation in the Last 10 Years J. Fusion Energy 40 3
- [9] Stangeby P C 1995 A problem in the interpretation of tokamak Langmuir probes when a fast electron component is present Plasma Phys. Control. Fusion 37 1031–7
- [10] Carr M et al., 2019 Physically principled reflection models applied to filtered camera imaging inversions in metal walled fusion machines Rev. Sci. Instrum. 90 043504
- [11] Perek A et al., 2022 A spectroscopic inference and SOLPS-ITER comparison of flux-resolved edge plasma parameters in detachment experiments on TCV Nucl. Fusion 62 096012
- [12] Song Y et al., 2023 Realization of thousand-second improved confinement plasma with Super I-mode in Tokamak EAST Sci. Adv. 9 eabq5273
- [13] Wen W et al., 2024 Progress of the bolometer diagnostic system on EAST Plasma Sci. Technol. 26 095102
- [14] Xu Z et al., 2016 Filterscope diagnostic system on the Experimental Advanced Superconducting Tokamak (EAST) Rev. Sci. Instrum. 87 11D429
- [15] Meng L Y et al., 2022 Development of Langmuir probe array for the new lower tungsten divertor in EAST Fusion Eng. Des. 175
- [16] Xu G S et al., 2023 Recent advances in developing natural and impurity-induced small/no-ELM H-mode regimes in EAST Rev. Mod. Plasma Phys. 7 14
- [17] Wüthrich C et al., 2025 Dependence of divertor turbulence on plasma density and current in TCV Nucl. Fusion 65 016011

- [18] Pan O et al., 2023 SOLPS-ITER simulations of an X-point radiator in the ASDEX Upgrade tokamak Nucl. Fusion 63 016001
- [19] Yu Y et al., 2025 Deep learning-enabled real-time prediction of impurity-induced detachment in EAST Plasma Phys. Control. Fusion 67 025026
- [20] Kinney J B and Atwal G S 2014 Equitability, mutual information, and the maximal information coefficient Proc. Natl. Acad. Sci.  $111\ 3354-9$
- [21] Luo D and Wang X 2024 ModernTCN: A Modern Pure Convolution Structure for General Time Series Analysis The Twelfth International Conference on Learning Representations International Conference on Learning Representations
- [22] Heinrich P et al., 2020 Self-sustained divertor oscillations in ASDEX Upgrade Nucl. Fusion 60 076013

